

Provided for non-commercial research and education use.
Not for reproduction, distribution or commercial use.



(This is a sample cover image for this issue. The actual cover is not yet available at this time.)

This article appeared in a journal published by Elsevier. The attached copy is furnished to the author for internal non-commercial research and education use, including for instruction at the authors institution and sharing with colleagues.

Other uses, including reproduction and distribution, or selling or licensing copies, or posting to personal, institutional or third party websites are prohibited.

In most cases authors are permitted to post their version of the article (e.g. in Word or Tex form) to their personal website or institutional repository. Authors requiring further information regarding Elsevier's archiving and manuscript policies are encouraged to visit:

<http://www.elsevier.com/copyright>



Contents lists available at SciVerse ScienceDirect

Mechanics Research Communications

journal homepage: www.elsevier.com/locate/mechrescom

Analytical solution of a semi-permeable crack in a 2D piezoelectric medium based on the PS model

CuiYing Fan^a, YanFei Zhao^c, MingHao Zhao^{a,b,*}, Ernian Pan^{a,c}^a The School of Mechanical Engineering, Zhengzhou University, Zhengzhou, Henan, 450001, PR China^b Department of Engineering Mechanics, Zhengzhou University, Zhengzhou, Henan, 450001, PR China^c Department of Civil Engineering, University of Akron, Ohio 44325, USA

ARTICLE INFO

Article history:

Received 22 June 2011

Received in revised form

22 November 2011

Available online xxx

Keywords:

Piezoelectric fracture

Dislocation density method

Polarization saturation (PS)

Semi-permeable crack

Intensity factor

ABSTRACT

This paper considers a straight but nonlinear crack in a two-dimensional piezoelectric plane. Different to the existing theoretical solution of the well-known polarization saturation (PS) model, we assume the crack to be semi-permeable. By introducing the dislocation density along the crack line, we derive the analytical solution for the field quantities. Numerical results show that the effect of different boundary conditions on the electric yielding zone and the stress intensity factor is significant and should not be ignored. The influence of the saturated electric displacement on the stress intensity factor and the electric displacement in the crack cavity is also demonstrated.

© 2012 Elsevier Ltd. All rights reserved.

1. Introduction

Due to the wide use of piezoelectric ceramics in smart structures, research on fracture of this type of materials becomes extremely important (i.e., Suo et al., 1992; Pan, 1999; Zhang et al., 2002; Jin and Zhong, 2002; Lin et al., 2003; Fang et al., 2004; Kuna, 2010; Zhong and Zhang, 2010). As is well known, the extension of the current fundamental fracture concepts or criteria in pure elasticity to piezoelectricity is not straightforward since the coupling between the mechanical and electric fields is complicated (Suo et al., 1992; Zhang et al., 2002).

Gao et al. (1997) extended the classical Dugdale model (Dugdale, 1960) to a strip polarization saturation (PS) model in piezoelectricity by assuming that the electric displacement is constant on a strip adjacent to a crack tip. The piezoelectric fields and fracture features predicted based on the PS model are in broad agreement with experimental observations (Park and Sun, 1995). McMeeking (2001) pointed out, from the energy point of view, that the PS model actually corresponds to a mechanical Dugdale model in which the strain remains constant. For this reason, Zhang et al. (2005) proposed a strip dielectric breakdown (DB) model assuming that the electric field strength should be constant in a strip adjacent to a

crack tip. It is found that the DB model gives the same results as the PS model in predicting the effects of an applied electric field on the fracture of piezoelectric media (Zhang et al., 2005). The study of the PS and DB models was also conducted by Ru and Mao (1999), Wang (2000), Beom et al. (2006), Loboda et al. (2010), Gao et al. (2006), among others. Recently, Fan et al. (2009) developed a numerical method, the nonlinear hybrid extended displacement discontinuity-fundamental solution (NHEDD-FS) method, where both the PS and DB models can be considered, to study the effect of the electric boundary condition on the field quantities. The numerical results by Fan et al. (2009) show that the electric displacement in the crack cavity was approximately constant and that the calculated result of the field quantities under the semi-permeable electric crack condition was very close to that under the impermeable condition for the given loadings and material parameters. However, the influence of the electric boundary condition on the fracture features could be significant as demonstrated by Loboda et al. (2010) and Fan et al. (2011), among others.

Several models were proposed in the literature to consider the effect of the electric field in the crack cavity, e.g., the self-consistent, energetically consistent, electrostatic traction (Zhang et al., 2002; Landis, 2004; Ricoeur and Kuna, 2009) and semi-permeable boundary conditions (Hao and Shen, 1994). Fan et al. (2011) studied these models and found that the self-consistent one would lead to almost the same result as the semi-permeable boundary condition model. As such, the simple boundary condition, i.e., the semi-permeable boundary condition will be adopted in this paper in order to obtain

* Corresponding author at: The School of Mechanical Engineering, Zhengzhou University, No. 100 Science Road, Zhengzhou, Henan Province, 450001, PR China. Tel.: +86 371 67781752; fax: +86 371 67781237.

E-mail addresses: memhzhao@sina.com, memhzhao@zzu.edu.cn (M. Zhao).

the analytical solution of the problem. In other words, in this paper, we assume a semi-permeable crack for the opening part of the crack and the PS model for the electric yielding zone (EYZ). The dislocation density concept is then applied to derive the integral equations. Simple numerical solutions of these equations show significant influence of the semi-permeable crack model on the field quantities as compared to the simple impermeable crack model. The paper is organized as follows: In Section 2, we present the basic equations; In Section 3, the semi-permeable as well as the impermeable crack models are described along with the corresponding boundary conditions; The boundary integral equations are derived in Section 4, and the expressions for the field intensity factors and local J-integral are given in Section 5; Numerical examples are carried out in Section 6, and conclusions are drawn in Section 7.

2. Basic equations

In the absence of body force and free electric charge, the extended equilibrium equations, geometric relations, and the constitutive relations of piezoelectric media are given by

$$\sigma_{ij,j} = 0, \quad D_{i,i} = 0, \quad i, j = 1, 2, 3 \text{ (or } x, y, z), \quad (1)$$

$$\varepsilon_{ij} = \frac{1}{2}(u_{i,j} + u_{j,i}), \quad E_i = -\varphi_{,i}, \quad (2)$$

$$\sigma_{ij} = C_{ijkl}\varepsilon_{kl} - e_{kij}E_k, \quad k, l = 1, 2, 3 \text{ or } x, y, z, \quad (3a)$$

$$D_k = e_{kij}\varepsilon_{ij} + \kappa_{kl}E_l, \quad (3b)$$

where σ_{ij} and D_i are the stresses and electric displacements, respectively; ε_{ij} and E_i are the strain and electric fields, respectively; $u_i (i=1-3)$ and $\varphi = u_4$ are the elastic displacements and the electric potential, respectively; and C_{ijkl} , e_{ijk} and κ_{ij} stand for the elastic constants, the piezoelectric constants and the dielectric constants, respectively. A subscript comma denotes the partial differentiation with respect to the coordinate after the comma.

For a generalized two-dimensional deformation in which the extended displacement vector $\mathbf{u} = (u_1 \ u_2 \ u_3 \ \varphi)^T$ and the extended stress function vector $\Phi = (\phi_1 \ \phi_2 \ \phi_3 \ \phi_4)^T$ depends only on x_1 and x_2 , the general solution takes the form (Suo et al., 1992; Zhang et al., 2002):

$$\mathbf{u} = \mathbf{A}\mathbf{f}(z) + \overline{\mathbf{A}\mathbf{f}(\bar{z})}, \quad (4a)$$

$$\Phi = \mathbf{B}\mathbf{f}(z) + \overline{\mathbf{B}\mathbf{f}(\bar{z})}, \quad (4b)$$

where $\mathbf{A} = (\mathbf{a}_1 \ \mathbf{a}_2 \ \mathbf{a}_3 \ \mathbf{a}_4)$ and $\mathbf{B} = (\mathbf{b}_1 \ \mathbf{b}_2 \ \mathbf{b}_3 \ \mathbf{b}_4)$ with \mathbf{a}_i and $\mathbf{b}_i (i=1, 2, 3, 4)$ being both the four-dimensional eigenvectors; $\mathbf{f}(z) = (f_1(z_1) \ f_2(z_2) \ f_3(z_3) \ f_4(z_4))^T$ is an analytic function vector; $z_i = x_1 + p_i x_2$ with p_i being the eigenvalue with a positive imaginary part. The eigenvalues and eigenvectors are determined by the following eigenvalue relations

$$[\mathbf{Q} + p(\mathbf{R} + \mathbf{R}^T) + p^2\mathbf{T}]\mathbf{A} = 0, \quad (5)$$

$$\mathbf{b}_i = [\mathbf{R}^T + p_i\mathbf{T}]\mathbf{a}_i = -\frac{1}{p_i}[\mathbf{R} + p_i\mathbf{T}]\mathbf{a}_i, \quad (6)$$

where

$$Q_{jk} = C_{1jk1}, \quad R_{jk} = C_{1jk2}, \quad T_{jk} = C_{2jk2}. \quad (7)$$

The extended stress vectors are calculated from the extended stress function vector:

$$\Sigma_2 = (\sigma_{21} \ \sigma_{22} \ \sigma_{23} \ D_2)^T = \Phi_{,1}, \quad (8)$$

$$\Sigma_1 = (\sigma_{11} \ \sigma_{12} \ \sigma_{13} \ D_1)^T = -\Phi_{,2}. \quad (9)$$

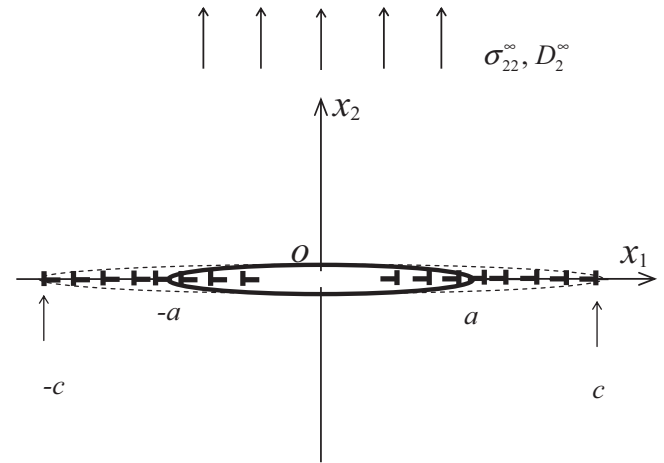


Fig. 1. Schematic of distributed dislocations along the crack line in the PS model where $|x_1| < a$ is the opening part of the crack and $a < |x_1| < c$ the electric yielding zone (EYZ).

In addition, matrix \mathbf{H} , which was defined in Zhang et al. (2005), will be used in the following analyses

$$\mathbf{H} = 2\text{Re}[i\mathbf{A}\mathbf{B}^{-1}], \quad \mathbf{H}^{-1} = \begin{pmatrix} \mathbf{F}_1 & \mathbf{F}_2^T \\ \mathbf{F}_2 & \mathbf{F}_{44} \end{pmatrix}, \quad (10)$$

where

$$\mathbf{F}_1 = \begin{pmatrix} F_{11} & F_{12} & F_{13} \\ F_{21} & F_{22} & F_{23} \\ F_{31} & F_{32} & F_{33} \end{pmatrix}, \quad \mathbf{F}_2 = (F_{41} \ F_{42} \ F_{43}), \quad (11)$$

and $F_{ij} (i, j = 1, 2, 3, 4)$ are material-related constants (Zhang et al., 2005).

3. The crack models and associated boundary conditions

Fig. 1 shows a crack S based on the PS model where the poling direction of the piezoelectric medium is along the x_2 -axis, $(-a, a)$ denotes the opening part of the crack, and $(-c, a)$ and (a, c) denote the electric yielding zone (EYZ). The external loading is applied uniformly at infinity,

$$\Sigma_2^\infty = (\sigma_{21}^\infty \ \sigma_{22}^\infty \ \sigma_{23}^\infty \ D_2^\infty)^T. \quad (12)$$

The extended boundary conditions on the crack surface for the general case require

$$\Sigma_2 = (\sigma_{21} \ \sigma_{22} \ \sigma_{23} \ D_2)^T = (0 \ 0 \ 0 \ D_2^c(x_1))^T, \quad -a < x_1 < a, \quad (13)$$

where D_2^c denotes the electric displacement in the crack cavity.

For an electrically impermeable crack model, we have

$$D_2^+(x_1) = D_2^-(x_1) = 0, \quad D_2^c(x_1) = 0, \quad (14)$$

where the superscripts “+” and “-” denote the upper and lower crack surfaces, respectively.

For a semi-permeable crack model, the electric displacement in the crack cavity along the crack is related to the crack opening displacement and electric potential jump by (Hao and Shen, 1994)

$$D_2^c(x_1) = -\kappa^c \frac{\varphi^+(x_1) - \varphi^-(x_1)}{u_2^+(x_1) - u_2^-(x_1)} = -\kappa^c \frac{|\varphi(x_1)|}{|u_2(x_1)|}, \quad (15)$$

where κ^c is the dielectric constant of the medium inside the opening crack, $|\varphi(x_1)| \equiv \varphi^+(x_1) - \varphi^-(x_1)$ is the potential jump, and $||u_2(x_1)|| \equiv u_2^+(x_1) - u_2^-(x_1)$ is the crack opening displacement.

Eqs. (13)–(15) give the boundary conditions in the opening part of the crack ($|x_1| \leq a$). Along the EYZ, we assume the PS model, which takes the following form (Gao et al., 1997),

$$u_i^+(x_1) = u_i^-(x_1), \quad D_2^+(x_1) = D_2^-(x_1) = D_S, \quad a < |x_1| < c, \quad i = 1, 2, 3, \quad (16)$$

where D_S is the saturated electric displacement.

4. Solutions in terms of integral equations

We will solve the crack problem described above via the integral equation method. We introduce four functions to represent the distributed dislocations, $g_i(x_1)$, which are actually associated with the Burgers vector components (the conventional elastic dislocations $\mathbf{b}^* = (b_1 \ b_2 \ b_3)$), and the electric dislocation $\Delta\varphi$ such that $g_i(x_1) b_i dx_1$ ($i = 1, 2, 3, 4$; with $b_4 \equiv \Delta\varphi$) represents the strength of the Burgers vector located at x_1 in the interval dx_1 . We now distribute the conventional dislocations from $-a$ to a , and the electric dislocation from $-c$ to c . Therefore, the crack opening displacements and the potential jump can be expressed by the extended dislocations, as

$$\begin{aligned} |u_i(x_1)| &= u_i^+(x_1) - u_i^-(x_1) = \int_{x_1}^a g_i(x'_1) b_i dx'_1, & |x_1| \leq a, \\ |\varphi(x_1)| &= \varphi^+(x_1) - \varphi^-(x_1) = \int_{x_1}^c g_4(x'_1) \Delta\varphi dx'_1, & |x_1| \leq c. \end{aligned} \quad (17)$$

Making use of the extended dislocation Green's functions (Zhang et al., 2005) and the boundary conditions in Eqs. (12) and (13), we derive the following integral equations for the general case (Eq. (13)) based on the PS model

$$\int_{-a}^a \frac{1}{\pi(x_1 - x'_1)} \mathbf{F}_1 \langle g_i \rangle \mathbf{b}^* dx'_1 + \int_{-c}^c \frac{1}{\pi(x_1 - x'_1)} \mathbf{F}_2^T g_4 \Delta\varphi dx'_1 + \mathbf{t}^* = 0, \quad |x_1| \leq a, \quad (18a)$$

$$\int_{-a}^a \frac{1}{\pi(x_1 - x'_1)} \mathbf{F}_2 \langle g_i \rangle \mathbf{b}^* dx'_1 + \int_{-c}^c \frac{1}{\pi(x_1 - x'_1)} F_{44} g_4 \Delta\varphi dx'_1 + D_2^\infty = D_2^c(x_1), \quad |x_1| \leq a, \quad (18b)$$

$$\int_{-a}^a \frac{1}{\pi(x_1 - x'_1)} \mathbf{F}_2 \langle g_i \rangle \mathbf{b}^* dx'_1 + \int_{-c}^c \frac{1}{\pi(x_1 - x'_1)} F_{44} g_4 \Delta\varphi dx'_1 + D_2^\infty = D_S, \quad a \leq |x_1| \leq c, \quad (18c)$$

where $\langle g_i(x_1) \rangle$ is a 3×3 diagonal matrix, and

$$\mathbf{t} = (\sigma_{12}^\infty \ \sigma_{22}^\infty \ \sigma_{32}^\infty \ D_2^\infty)^T, \quad \mathbf{t}^* = (\sigma_{12}^\infty \ \sigma_{22}^\infty \ \sigma_{32}^\infty)^T. \quad (19)$$

Generally speaking, the potential jump $|\varphi(x_1)|$ and the crack opening displacement $|u_2(x_1)|$ depend on the location along the crack surface. As such, $D_2^c(x_1)$ in Eq. (15) or in Eq. (18b) would generally be the function of x_1 .

However, for a given loading, the crack opening displacement and the potential jump are approximately proportional to each other. Therefore, to the first-order approximation, the electric displacement D_2^c within the opening part of crack can be assumed as constant, except for points near the crack tip (Fan et al., 2009; Loboda et al., 2010). This approximation will be validated numerically later on.

From Eqs. (18a) and (18b), we can obtain

$$\int_{-a}^a \frac{1}{\pi(x_1 - x'_1)} \mathbf{F}_1^* \langle g_i \rangle \mathbf{b}^* dx'_1 + \mathbf{T}^* = 0, \quad |x_1| \leq a, \quad (20)$$

where

$$\mathbf{F}_1^* = \mathbf{F}_1 - \frac{\mathbf{F}_2^T \mathbf{F}_2}{F_{44}}, \quad \mathbf{T}^* = \mathbf{t}^* - \left(\frac{\mathbf{F}_2^T}{F_{44}} \right) (D_2^\infty - D_2^c). \quad (21)$$

Thus, the solution to Eq. (20) is given by

$$\langle g_i \rangle \mathbf{b}^* = \mathbf{F}_1^{*-1} \mathbf{T}^* \frac{x_1}{(a^2 - x_1^2)^{1/2}}, \quad |x_1| \leq a. \quad (22)$$

From Eqs. (18b) and (18c), we derive the following dual integral equations

$$\int_{-c}^c \frac{1}{\pi(x_1 - x'_1)} (\mathbf{F}_2 \langle g_i \rangle \mathbf{b}^* + F_{44} g_4 \Delta\varphi) dx'_1 + D_2^\infty - D_2^c = 0, \quad |x_1| \leq a, \quad (23a)$$

$$\int_{-c}^c \frac{1}{\pi(x_1 - x'_1)} (\mathbf{F}_2 \langle g_i \rangle \mathbf{b}^* + F_{44} g_4 \Delta\varphi) dx'_1 + D_2^\infty - D_2^c = D_S - D_2^c, \quad a \leq |x_1| \leq c, \quad (23b)$$

where

$$\langle g_i \rangle \mathbf{b}^* = \begin{cases} \mathbf{F}_1^{*-1} \mathbf{T}^* \frac{x_1}{(a^2 - x_1^2)^{1/2}}, & |x_1| \leq a, \\ 0 & a < |x_1| < c, \end{cases} \quad (24)$$

Using the Muskhelishvili method (Muskhelishvili, 1953), we find the solution of Eqs. (23a) and (23b) as

$$\mathbf{F}_2 \langle g_i \rangle \mathbf{b}^* + F_{44} g_4 \Delta\varphi = \frac{D_S - D_2^c}{\pi} \left[ch^{-1} \left| \frac{c^2 - ax_1}{c(a - x_1)} \right| - ch^{-1} \left| \frac{c^2 + ax_1}{c(a + x_1)} \right| \right]. \quad (25)$$

We therefore have

$$g_4 \Delta\varphi = \begin{cases} \frac{D_S - D_2^c}{F_{44}\pi} \left[ch^{-1} \left| \frac{c^2 - ax_1}{c(a - x_1)} \right| - ch^{-1} \left| \frac{c^2 + ax_1}{c(a + x_1)} \right| \right] - \frac{\mathbf{F}_2 \mathbf{F}_1^{*-1} \mathbf{T}^*}{F_{44}} \frac{x_1}{(a^2 - x_1^2)^{1/2}}, & |x_1| \leq a, \\ \frac{D_S - D_2^c}{F_{44}\pi} \left[ch^{-1} \left| \frac{c^2 - ax_1}{c(a - x_1)} \right| - ch^{-1} \left| \frac{c^2 + ax_1}{c(a + x_1)} \right| \right], & a < |x_1| < c. \end{cases} \quad (26)$$

Up to now, the size of the EYZ c and the electric displacement D_2^c are still unknowns, and thus extra conditions are needed to obtain the final solutions. From Eq. (15) for the semi-permeable crack model, the electric displacement D_2^c in the crack cavity is related to the crack opening displacement and the potential jump. Based on the PS model for piezoelectric media (Gao et al., 1997), we know that the electric displacement has no singularity at the tip of the EYZ. Therefore, in order to satisfy the non-singularity of electric displacement at $|x_1| = c$, we require that for a given D_2^c , similar to the DB model and PS model (Gao et al., 1997; Wang, 2000; Zhang et al., 2005), the following equation be satisfied

$$\frac{c}{a} = \sec \left(\frac{\pi (D_2^\infty - D_2^c)}{2(D_S - D_2^c)} \right), \quad (27)$$

which determines the size of the EYZ.

For the impermeable crack model (Eq. (14)), we have $D_2^c = 0$, and thus the size of the EYZ from Eq. (27) is reduced to

$$\frac{a}{c} = \cos\left(\frac{\pi D_2^\infty}{2D_5}\right), \quad (28)$$

which is the same as in Gao et al. (1997) and Wang (2000). In other words, Eq. (27) extends the non-singularity condition in the impermeable crack model to the general crack surface loading case.

Substituting Eq. (27) into Eq. (26) and Eq. (17), the crack opening displacement and the potential jump at an arbitrary point $(x_1, 0)$ along the crack surface and on the EYZ can be expressed in terms of the extended dislocation. Then, substituting the crack opening displacement and the potential jump into Eq. (15), we obtain the electric displacement D_2^c at any point $(x_1, 0)$ along the crack

$$\frac{D_2^c}{\kappa^c} = -\frac{1}{\pi F_{44}[\mathbf{F}_1^{-1}\mathbf{T}^*]_2} \left(\frac{(D_5 - D_2^c)[M_1(D_5, x_1) - M_2(D_5, x_1)]}{M_3(x_1)} - \pi \mathbf{F}_2 \mathbf{F}_1^{-1} \mathbf{T}^* \right), \quad (29)$$

$|x_1| \leq a,$

where $[\mathbf{F}_1^{-1}\mathbf{T}^*]_2$ denotes the second row of the matrix, and

$$M_1(D_5, x_1) = \int_{x_1}^c \left[ch^{-1} \left| \frac{c^2 - ax'_1}{c(a - x'_1)} \right| \right] dx'_1, \quad (30a)$$

$$M_2(D_5, x_1) = \int_{x_1}^c \left[ch^{-1} \left| \frac{c^2 + ax'_1}{c(a + x'_1)} \right| \right] dx'_1, \quad (30b)$$

$$M_3(x_1) = \sqrt{a^2 - x_1'^2}. \quad (30c)$$

Eq. (29) is used to determine the electric displacement D_2^c in the crack cavity for the semi-permeable crack model. It is obvious that, under the condition Eq. (15), the electric displacement would be, in general, not constant but the function of x_1 . As stated before, we assume it to be a constant in this paper. Substituting the derived D_2^c in Eq. (29) into Eq. (27), we finally obtain the EYZ.

5. Field intensity factors and local J-integral

The stress in front of the crack tip on the x_1 -axis is calculated by

$$\begin{aligned} \Sigma_2 \equiv (\sigma_{21} \ \sigma_{22} \ \sigma_{23} \ D_2)^T &= \int_{-a}^a \frac{1}{\pi(x_1 - x'_1)} \begin{pmatrix} \mathbf{F}_1 \\ \mathbf{F}_2 \end{pmatrix} \langle g_i(x'_1) \rangle \mathbf{b}^* dx'_1 \\ &+ \int_{-c}^c \frac{1}{\pi(x_1 - x'_1)} \begin{pmatrix} \mathbf{F}_2^T \\ F_{44} \end{pmatrix} g_4(x'_1) \Delta\phi dx'_1 \\ &+ \mathbf{t}. \end{aligned} \quad (31)$$

Defining the field intensity factor vector,

$$\mathbf{K} = \lim_{x_1 \rightarrow a} \sqrt{2\pi(x_1 - a)} \Sigma_2, \quad (32)$$

we obtain the local field intensity factor vector as

$$\mathbf{K}^{(l)} = \begin{pmatrix} K_{II}^{(l)} & K_I^{(l)} & K_{III}^{(l)} & K_D^{(l)} \end{pmatrix}^T = \sqrt{\pi a} \left[\begin{pmatrix} \mathbf{F}_1 \\ 0 \end{pmatrix} - \begin{pmatrix} \mathbf{F}_2^T \\ 0 \end{pmatrix} \frac{\mathbf{F}_2}{F_{44}} \right] \mathbf{F}_1^{-1} \mathbf{T}^*, \quad (33)$$

which can be further written as

$$\mathbf{K}^{(l)} = \begin{pmatrix} K_{II}^{(a)} \\ K_I^{(a)} \\ K_{III}^{(a)} \\ 0 \end{pmatrix} - \frac{1}{F_{44}} \begin{pmatrix} F_{41}K_D^{(a)} \\ F_{42}K_D^{(a)} \\ F_{43}K_D^{(a)} \\ 0 \end{pmatrix} + \frac{1}{F_{44}} \begin{pmatrix} F_{41}K_{Dc} \\ F_{42}K_{Dc} \\ F_{43}K_{Dc} \\ 0 \end{pmatrix}, \quad (34)$$

where

$$\begin{pmatrix} K_{II}^{(a)} & K_I^{(a)} & K_{III}^{(a)} & K_D^{(a)} \end{pmatrix}^T = \sqrt{\pi a} \begin{pmatrix} \sigma_{12}^\infty & \sigma_{22}^\infty & \sigma_{32}^\infty & D_2^\infty \end{pmatrix}^T, \quad (35)$$

$$K_{Dc} = \sqrt{\pi a} D_2^c.$$

We point out again that Eq. (34) is the solution of the local field intensity factor and that there are three sources contributing to it: the first term on the right-hand side of Eq. (34) is related to the far-field mechanical loading, the second to the far-field electric displacement loading, and finally the third term to the electric displacement in the crack cavity. It can be easily shown that if $D_2^c = 0$ and $K_{Dc} = 0$, Eq. (34) reduces to the solutions for the impermeable crack model as in Wang (2000) and Fan et al. (2009).

For the piezoelectric medium, the J -integral is related to the field intensity factor as (Zhang et al., 2005)

$$J = \mathbf{K}^T \frac{\mathbf{H}}{4} \mathbf{K}. \quad (36)$$

Therefore, substituting Eq. (34) into Eq. (36) yields the local J -integral $J^{(l)}$ of the piezoelectric medium as

$$J^{(l)} = \mathbf{K}^{(l)T} \frac{\mathbf{H}}{4} \mathbf{K}^{(l)}. \quad (37)$$

Since the last term on the right-hand side of Eq. (34) is the contribution of the electric displacement D_2^c in the crack cavity to the local intensity factor, it can be seen, from Eqs. (29), (34) and (37), that the local field intensity factor and local J -integral are related not only to the material coefficients and the applied far-field, but also to the saturated electric displacement D_5 . This is the major observation which has not been reported in existing literature.

6. Numerical examples

To investigate the effect of the electric displacement in the crack cavity on the piezoelectric fracture, we numerically calculate the size of the EYZ and the local stress intensity factor under different crack boundary conditions (semi-impermeable and impermeable crack models). Two types of far-field loadings are considered: mechanical loading $\sigma_{22}^\infty \equiv \sigma$ and electric loading $D_2^\infty \equiv D$. We take a finite crack in an infinite PZT-4 piezoelectric material as an example with the material properties being listed in Table 1. The dielectric constant of the material in the crack cavity is taken to be $\kappa^c = 8.85 \times 10^{-12} \text{ Fm}^{-1}$. Two cases are studied: one with fixed D_5 and the other with varying D_5 .

6.1. Results based on different boundary conditions with fixed saturated electric displacement

We first assume that the saturated electric displacement is $D_5 = 0.2 \text{ C/m}^2$. Fig. 2 shows the electric displacement in the crack cavity calculated using Eq. (15). It can be seen that under different mechanical $\sigma_{22}^\infty \equiv \sigma$ and electric $D_2^\infty \equiv D$ loadings, the electric displacement in the crack cavity is indeed constant except for the region near the crack tip. This result validates the assumption we made on the electric displacement. Therefore, in the following calculation, we take the electric displacement at the center (0,0) of the crack as the uniform value in the crack cavity.

Figs. 3 and 4 show the EYZ size versus the far-field mechanical and electric loadings for both semi-permeable and impermeable crack models. These two figures clearly demonstrate the influence of different crack surface conditions on the EYZ size. It is observed from Fig. 3 that under a relatively small mechanical load (with fixed far-field electric displacement), the EYZ size of a semi-impermeable crack model is usually smaller than that of the impermeable crack model (the EYZ size of the impermeable crack is independent of the mechanical load). However, with increasing mechanical load, the EYZ size of the semi-permeable crack

Table 1
Material properties of PZT-4.

Elastic constant (10^9 N/m ²)					Piezoelectric constant (C/m ²)			Dielectric constant (10^{-9} F/m)	
C_{11}	C_{33}	C_{44}	C_{13}	C_{12}	e_{15}	e_{31}	e_{33}	κ_{11}	κ_{33}
139	113	25.6	74.3	77.8	13.4	-6.98	13.8	6.0	5.47

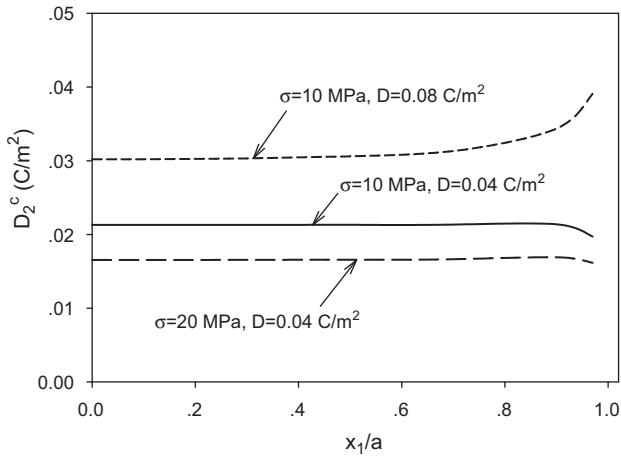


Fig. 2. Variation of the electric displacement in the crack cavity along the crack using Eq. (15).

increases and eventually reaches the EYZ size of the impermeable crack (at around $\sigma = 450$ MPa). With further increase of the far-field mechanical load, the electric displacement in the crack cavity becomes negative for the semi-permeable crack (as shown in the inserted figure in Fig. 3), which means that the electric potential jump is in the opposite direction. Fig. 4 shows the corresponding EYZ size versus the applied far-field electric displacement for both crack models. It is interesting that the EYZ size of the impermeable and semi-permeable cracks increases monotonically with increasing far-field electric displacement. It is noted that, under a small electric loading (e.g., $D < 0.025$ or $< 12.5\%$ of D_S), the electric displacement in the crack cavity corresponding to the semi-permeable crack could not be determined (as shown in the inserted figure for the regular part only). The reason is unclear yet.

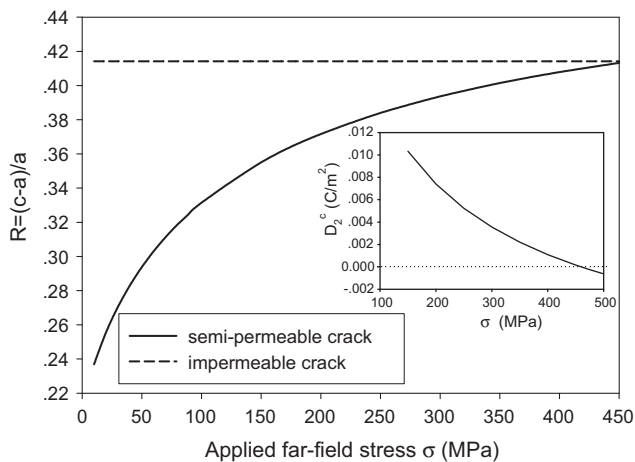


Fig. 3. Size of the electric yielding zone (EYZ) versus the mechanical loading $\sigma_{22}^\infty = \sigma$ for semi-permeable and impermeable crack models with fixed $D_2^\infty = D = 0.1$ C/m² and $D_5 = 0.2$ C/m². Inserted figure shows the electric displacement in the crack cavity versus the mechanical loading.

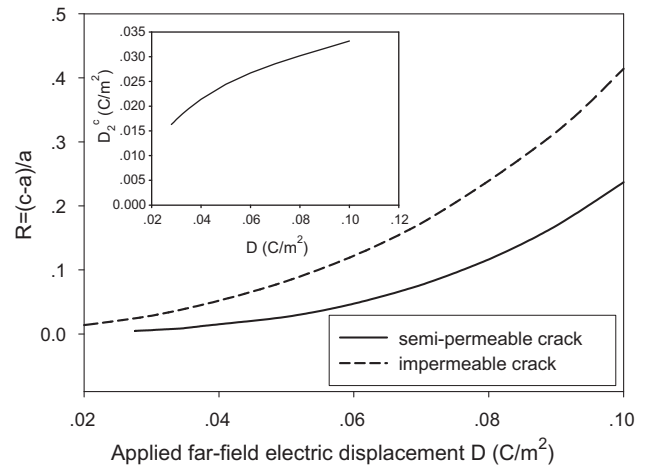


Fig. 4. Size of the electric yielding zone (EYZ) versus the electric loading $D_2^\infty = D$ for semi-permeable and impermeable crack models with fixed $\sigma_{22}^\infty = \sigma = 10$ MPa and $D_5 = 0.2$ C/m². Inserted figure shows the electric displacement in the crack cavity versus the electric loading.

Figs. 5 and 6 display the stress intensity factor (SIF) versus the electric and mechanical loads for both crack models. The normalized local stress intensity factor is given by

$$K_I^* = \frac{K_I^{(l)}}{\sqrt{\pi a \sigma_{22}^\infty}} \quad (38)$$

It is observed from Fig. 5 that for a given mechanical load, the normalized SIF corresponding to the impermeable crack is larger than that corresponding to the semi-permeable crack and that the SIFs in both crack models decrease monotonically with increasing far-field mechanical load. They both reach the same asymptotical value (about 1.4) under a large mechanical load. This interesting feature implies that, under a relatively large mechanical load

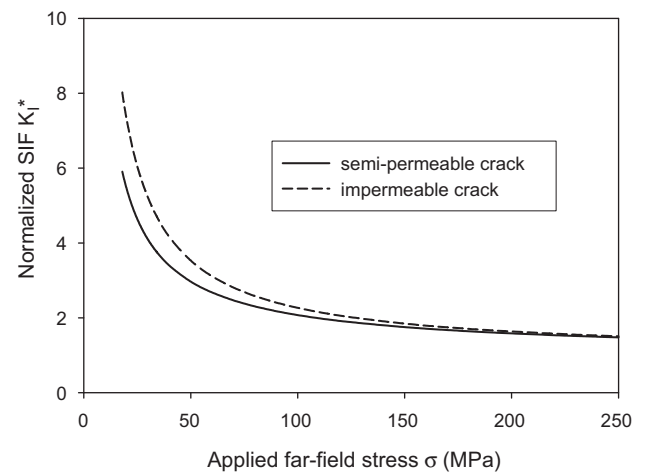


Fig. 5. Normalized stress intensity factor (SIF) versus the mechanical loading $\sigma_{22}^\infty = \sigma$ for semi-permeable and impermeable crack models with fixed $D_2^\infty = D = 0.1$ C/m² and $D_5 = 0.2$ C/m².

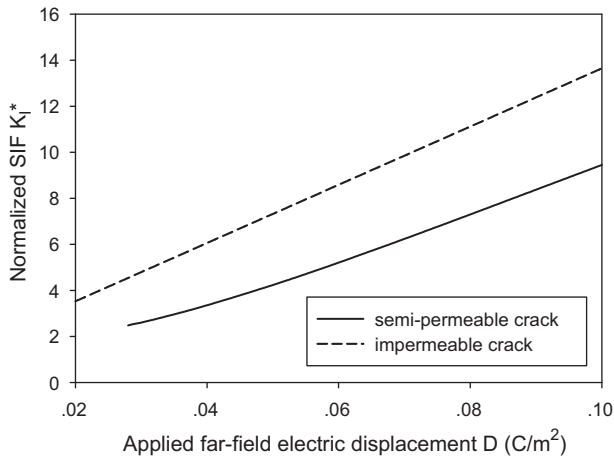


Fig. 6. Normalized stress intensity factor (SIF) versus the electric loading $D_2^\infty \equiv D$ for semi-permeable and impermeable crack models with fixed $\sigma_{22}^\infty \equiv \sigma = 10$ MPa and $D_S = 0.2C/m^2$.

(say >150 MPa), the simple impermeable crack model can be safely employed to calculate the normalized SIF (with a relative error less than 5%) for $D_2^\infty \equiv D = 0.1C/m^2$ and $D_S = 0.2C/m^2$. Fig. 6 shows the variation of the normalized SIF with the applied far-field electric displacement. It is obvious that for a given electric displacement, the SIF of the impermeable crack is much larger than that of the semi-permeable crack. However, the SIF for impermeable crack increases linearly with electric displacement, while the SIF for semi-permeable crack varies nonlinearly with electric displacement under the relatively small electric load.

It is observed from Figs. 3–6 that the difference between the results based on the semi-permeable crack and the impermeable crack is significant. This demonstrates that the effect of the electric field in the crack cavity cannot be ignored except for the case of large mechanical load. These nonlinear features are different from those associated with the impermeable crack (Wang, 2000).

6.2. Influence of saturated electric displacement

Fig. 7 displays, for a semi-permeable crack model, the electric displacement D_2^c in the crack cavity versus the saturated electric displacement D_S for different far-field electric displacements but with fixed far-field mechanical load $\sigma_{22}^\infty \equiv \sigma = 10$ MPa. It is obvious that for a given saturated electric displacement, the electric

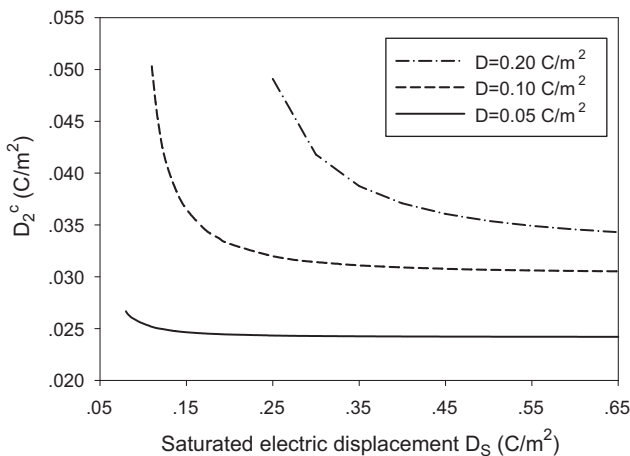


Fig. 7. Electric displacement D_2^c in the semi-permeable crack cavity versus the saturated electric displacement D_S with fixed $\sigma_{22}^\infty \equiv \sigma = 10$ MPa.

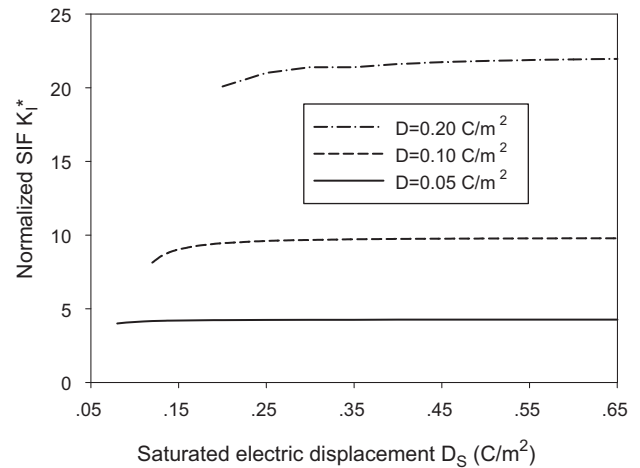


Fig. 8. Normalized stress intensity factor (SIF) versus saturated electric displacement D_S for the semi-permeable crack with fixed $\sigma_{22}^\infty \equiv \sigma = 10$ MPa.

displacement D_2^c in the crack cavity decreases with decreasing far-field D , and that for a given D , the electric displacement D_2^c decreases with increasing saturated electric displacement D_S (approaches asymptotically a limit value for larger D_S). It is further observed from Fig. 7 that the electric displacement D_2^c in the crack cavity is singular when $D_2^\infty = D_S$. Fig. 8 displays the normalized SIF of the semi-permeable crack versus saturated electric displacement D_S . It is seen from Fig. 8 that the normalized SIF slightly increases with increasing D_S and that there is a singularity in the SIF when the far-field electric displacement is close to certain value of D_S .

7. Concluding remarks

We have proposed a semi-permeable polarization saturation (PS) model. This relatively real boundary value problem of the crack is solved via the integral equation approach by introducing the dislocation density along the crack. Comparing to the simple impermeable crack model, our numerical results show clearly that, under either a far-field mechanical or electric load, the effect of different crack boundary conditions on the size of the electric yielding zone and the stress intensity factor is significant and should not be ignored in the piezoelectric fracture analysis. The influence of the saturated electric displacement on the stress intensity factor and on the electric displacement in the crack cavity is presented for the first time.

We further point out that the proposed approach can be extended to include other nonlinear electric boundary conditions, e.g., the electrostatic traction. However, in so doing, the quadratic terms of D_2^c would appear in the boundary condition, which makes the analytical solution more difficult, if not impossible. This problem will be attacked in the future via the numerical approaches, e.g., the extended displacement discontinuity method.

Acknowledgements

The work was supported by the National Natural Science Foundation of China (No. 10872184, No. 11102186 and No. 11072221), the Program for Innovative Research Team (in Science and Technology) in University of Henan Province (2010IRTSTHN013), and the Bairen Program in Henan Province. The authors would also like to thank the two reviewers for their constructive comments.

References

- Beom, H.G., Kim, Y.H., Cho, C., Kim, C.B., 2006. Asymptotic analysis of an impermeable crack in an electrostrictive material subjected to electric loading. *Int. J. Solids Struct.* 43, 6869–6886.
- Dugdale, D.S., 1960. Yielding of steel sheets containing slits. *J. Mech. Phys. Solids* 8, 100–104.
- Fan, C.Y., Zhao, M.H., Meng, L.M., Gao, C.F., Zhang, T.Y., 2011. On the self-consistent analysis, the energetically consistent approach, and electrostatic tractions in piezoelectric fracture mechanics. *Eng. Fract. Mech.* 48, 2373–2382.
- Fan, C.Y., Zhao, M.H., Zhou, Y.H., 2009. Numerical solution of polarization saturation/dielectric breakdown model in 2D finite piezoelectric media. *J. Mech. Phys. Solids* 57, 1527–1544.
- Fang, D.N., Wan, Y.P., Soh, A.K., 2004. Magnetoelastic fracture of soft ferromagnetic materials. *Theor. Appl. Fract. Mech.* 42, 317–334.
- Gao, C.F., Noda, N., Zhang, T.Y., 2006. Dielectric breakdown model for a conductive crack and electrode in piezoelectric materials. *Int. J. Eng. Sci.* 44 (3–4), 256–272.
- Gao, H., Zhang, T.Y., Tong, P., 1997. Local and global energy release rates for an electrically yielded crack in a piezoelectric ceramic. *J. Mech. Phys. Solids* 45, 491–510.
- Hao, T.H., Shen, Z.Y., 1994. A new electric boundary condition of electric fracture mechanics and its applications. *Eng. Fract. Mech.* 47, 793–802.
- Jin, B., Zhong, Z., 2002. A moving mode-III crack in functionally graded piezoelectric material: permeable problem. *Mech. Res. Commun.* 29, 217–224.
- Kuna, M., 2010. Fracture mechanics of piezoelectric materials – where are we right now? *Eng. Fract. Mech.* 77, 309–326.
- Landis, C.M., 2004. Energetically consistent boundary conditions for electromechanical fracture. *Int. J. Solids Struct.* 41, 6291–6315.
- Lin, S., Narita, F., Shindo, Y., 2003. Electroelastic analysis of a penny-shaped crack in a piezoelectric ceramic under mode I loading. *Mech. Res. Commun.* 30, 371–386.
- Loboda, V., Lapusta, Y., Sheveleva, A., 2010. Limited permeable crack in an interlayer between piezoelectric materials with different zones of electric saturation and mechanical yielding. *Int. J. Solids Struct.* 47, 1796–1806.
- McMeeking, R.M., 2001. Towards a fracture mechanics for brittle piezoelectric and dielectric materials. *Int. J. Fract.* 108, 25–41.
- Muskhelishvili, N.I., 1953. *Singular Integral Equations*. Noordhoff, Groningen.
- Pan, E., 1999. A BEM analysis of fracture mechanics in 2D anisotropic piezoelectric solids. *Eng. Anal. Bound. Elem.* 23, 67–76.
- Park, S.B., Sun, C.T., 1995. Fracture criteria for piezoelectric ceramics. *J. Am. Ceram. Soc.* 78, 1475–1480.
- Ricoeur, A., Kuna, M., 2009. Electrostatic tractions at crack faces and their influence on the fracture mechanics of piezoelectrics. *Int. J. Fract.* 157, 3–12.
- Ru, C.Q., Mao, X., 1999. Conducting crack in a piezoelectric ceramics of limited electrical polarization. *J. Mech. Phys. Solids* 47, 2125–2146.
- Suo, Z., Kuo, C.M., Barnett, D.M., Willis, J.R., 1992. Fracture mechanics for piezoelectric ceramics. *J. Mech. Phys. Solids* 40, 739–765.
- Wang, T.C., 2000. Analysis of strip electric saturation model of crack problem in piezoelectric materials. *Int. J. Solids Struct.* 37, 6031–6049.
- Zhang, T.Y., Zhao, M.H., Cao, C.F., 2005. The strip dielectric breakdown model. *Int. J. Fract.* 132, 311–327.
- Zhang, T.Y., Zhao, M.H., Tong, P., 2002. Fracture of piezoelectric ceramics. *Adv. Appl. Mech.* 38, 147–289.
- Zhong, X.C., Zhang, K.S., 2010. Electroelastic analysis of an electrically dielectric Griffith crack in a piezoelectric layer. *Int. J. Eng. Sci.* 48, 612–623.